AJNR Am J Neuroradiol 24:567–578, April 2003

CT and MR Imaging Findings and Their Implications in the Follow-up of Patients with Intracranial Aneurysms Treated with Endosaccular Occlusion with Onyx

Isil Saatci, H. Saruhan Cekirge, Elisa F. M. Ciceri, Michel E. Mawad, A. Gulsun Pamuk, and Aytekin Besim

BACKGROUND AND PURPOSE: **Our purpose was to describe the CT and MR features of intracranial aneurysms occluded with the liquid polymer Onyx.**

METHODS: **At two centers, 35 aneurysms in 33 patients and 11 in nine patients were treated with the polymer. In 17 patients, adjunctive stents were placed at the aneurysm neck. All but three aneurysms originated from the internal carotid artery (ICA). Eighteen were giant; 15, large; and 13, small. Patients underwent pre- and postprocedural CT and/or MR imaging; MR angiograms (MRAs) were available in 22. In 35 patients (38 aneurysms), 3-month and/or 1-year follow-up angiograms were obtained for correlation with sectional images.**

RESULTS: **Except in two small aneurysms, polymer filling created beam hardening artifacts on CT scans. In 10 aneurysms, the polymer did not fill the aneurysm sac entirely; five showed recanalization at follow-up. On MR images (all sequences), the polymer appeared hypointense, probably because of its tantalum content; it did not create artifacts. MRAs falsely suggested reduced or absent ICA flow in 11 of 22 patients, nine of whom with stents. In the rest, MRA provided results comparable to those of selective angiography. In 12 patients, postprocedural imaging revealed new lesions.**

CONCLUSION: **Onyx appears hypointense on MR images, with no artifact, and it does not interfere with MRA except in patients with stents. MR imaging may reveal new parenchymal lesions, even in asymptomatic patients. In the immediate control and follow-up of polymer-treated aneurysms, MR imaging and MRA may be preferred. CT may show the degree of filling in the aneurysmal sac, but Onyx creates artifacts that hinder CT evaluation.**

Many techniques are used for the treatment of intracranial aneurysms. In addition to surgical clipping, endovascular techniques such as parent-artery occlusion, coiling with or without auxiliary devices (eg, balloons for remodeling techniques and stents), or stenting alone are proven to be effective treatment options (1–6). However, recanalization is the major problem in many of these treatment alternatives, especially in wide-necked and fusiform aneurysms (7–9). Liquid agents have long been considered for use in endosaccular aneurysm occlusion, despite that control of their deposition can hardly be presumed (10). Onyx (formerly Embolyx; Micro Therapeutics, Inc, Irvine, CA) is a mixture of ethylene vinyl alcohol (EVOH), dimethyl sulfoxide (DMSO), and tantalum. Some have started to use this material for the treatment of intracranial arteriovenous malformations (AVMs) and for tumor embolization; initial results have already been presented (10–12). This treatment now seems to provide a safe alternative for the exclusion of the aneurysm from the circulation (13–14), though to our knowledge, effectiveness and long-term results have not yet been published.

The CT and MR imaging findings in patients with intracranial aneurysms treated with this polymer are described in this article. Because the use of this material began only recently, its imaging features are not known. In addition, follow-up of these patients must be well tailored because most of the aneurysms are the most difficult to treat, and they have an increased

Received July 11, 2002; accepted after revision November 7.

From the Departments of Radiology (I.S., H.S.C., A.B.) and Anesthesiology and Reanimation (A.G.P.); Hacettepe University Hospital, Ankara, Turkey; the Instituto Neurologico C. Besta, Milan, Italy (E.F.M.C.); and Department of Radiology, Methodist Hospital, Baylor College of Medicine, Houston, TX (M.E.M.).

Address reprint requests to Isil Saatci MD, Hacettepe University Hospital, Radiology Department, Sihhiye 06100, Ankara, Turkey.

Patient data

Patient, Aneurysm Location and Size*	Calcification	Thrombus	Mass Effect†	Tx/Repeat Tx‡	Examinations after First Tx		New Lesion¶	Follow-Up Angiography#	Recanalization**	MRA††
					CT§	MR Imaging‖				
1, R sc ICA, giant	Yes	Yes	Yes	Onyx16/ Onyx20 + S	2	3 (M)	No	Yes	Yes	Yes
2, R cav ICA, giant	Yes	No	Yes	Onyx20 + S/none	2	3 (M)	No	Yes	No	Yes
3										
R cav ICA, small	No	No	No	Onyx20/onyx20	2	2 (NI)	No	Yes	Yes	Yes
R cav ICA, small	No	No	No	Onyx20/none	2	2 (NI)	No	Yes	No	Yes
4, R pcav ICA, giant	No	Yes	Yes	Onyx20 + S/none	1	1 (M)	Asymptomatic	No	NA	No
5, L cav ICA, large	No	No	No	Onyx20 + S/none	1	2 (H)	No	Yes	No	Yes
6, R sc ICA, small	No	No	No	Onyx20/none	1	1 (H)	No	Yes	No	Yes
7, R sc ICA, small	No	No	No	Onyx20/none	1	2 (H)	No	Yes	No	Yes
8, L cav ICA, large	No	No	No	Onyx20 + S/none	1	2 (M)	No	Yes	No	Yes
9, L sc ICA, small	No	No	No	Onyx20/none	1	1 (H)	Asymptomatic	Yes	Yes	Yes
10, L cav ICA, small	No	No	No	Onyx20/none	1	1 (NI)	No	Yes	No	No
11, L pcav ICA, giant	Yes	Yes	Yes	Onyx16/onyx20 + S	1	2 (M)	No	Yes	Yes	No
12, R cav ICA, giant	Yes	Yes	Yes	Onyx20 + S/none	1	2 (M)	No	Yes	No	Yes
13, L sc ICA, large	No	No	No	Onyx20 + S/none	1	0 (NA)	Hemorrhage	No	NA	No
14										
Basilar tip, large	No	Yes	Yes	Onyx16/none	1	0 (NA)	No	No	NA	No
R sup cb, small	No	No	No	Onyx16/none	1	0 (NA)	No	No	NA	No
15, L sc ICA, large	No	No	No	Onyx20 + S/none	1	2 (H)	No	Yes	No	Yes
16, R p ICA, small	No	No	No	Onyx20 + S/none	1	1 (H)	No	No	NA	No
17, L sc ICA, giant	No	No	No	Onyx16/none	1	1 (H)	WS ischemia	Yes	No	Yes
18, R cav ICA, giant	Yes	Yes	No	Onyx20 + S/none	1	0 (NA)	WS ischemia	No	NA	No
19, R cav ICA, giant	No	Yes	No	Onyx16/none	2	0 (NA)	No	Yes	Yes	No
20, R cav ICA, large	No	No	No	Onyx16/none	2	0 (NA)	No	Yes	No	No
21, R sup cb, giant	Yes	Yes	Yes	Onyx16/none	1	2 (M)	Asymptomatic	Yes	Yes	No
22, R sc ICA, giant	Yes	Yes	Yes	Onyx20/onyx20 + S	3	2 (M)	No	Yes	Yes	Yes
23										
L sc ICA, giant	No	No	No	Onyx20/none	1	0 (NA)	No	Yes	No	No
R cav ICA, small	No	No	No	Onyx20/none	1	0 (NA)	No	Yes	No	No
R sc ICA, small	No	No	No	Onyx20/none	1	0 (NA)	No	Yes	No	No
24, R sc ICA, small	No	No	No	Onyx20/none	1	0 (NA)	No	No	NA	No
25, L cav ICA, large	No	No	No	Onyx20/none	1	0 (NA)	No	No	NA	No
26, R pcav ICA, large	No	No	No	Onyx20 + S/none	0	1 (M)	No	Yes	No	Yes
27, R cav ICA, giant	No	No	Yes	Onyx16/none	1	1 (M)	Transient CCF	Yes	No	No
28, R cav ICA, giant	No	No	Yes	Onyx20 + S/none	1	2 (M)	Asymptomatic	Yes	No	Yes
29, R cav ICA, giant	No	No	Yes	Onyx20 + S/none	0	1 (M)	No	Yes	No	No
30, R sc ICA, large	No	No	No	Onyx20/none	1	1 (H)	Asymptomatic	Yes	No	Yes
31, R cav ICA, small	No	No	No	Onyx20/none	0	1 (NI)	No	Yes	No	Yes
32, R sc ICA, giant	No	No	No	Onyx20 + S/none	1	2 (H)	Asymptomatic	Yes	No	Yes
33, R sc ICA, large	No	No	No	Onyx20/none	1	1 (H)	Asymptomatic	Yes	No	No
34, L sc ICA, large	No	No	No	Onyx20/none	1	1 (H)	No	Yes	No	Yes
35, L pc ICA, large	No	Yes	No	Onyx20/onyx20 + S	1	1 (M)	No	Yes	Yes	No
36, L sc ICA, large	No	No	Yes	Onyx20/none	1	0 (NA)	No	Yes	No	No
37, L sc ICA, small	No	No	No	Onyx20/none	0	2 (H)	No	Yes	No	Yes
38, L sc ICA, giant	No	Yes	Yes	Onyx20/none	1	2 (M)	Asymptomatic	Yes	No	Yes
39, L pc ICA, large	No	No	No	Onyx20/none	0	1 (M)	No	Yes	No	No
40, R sc ICA, giant	No	No	No	Onyx20/none	0	2 (M)	No	Yes	No	Yes
41, L sc ICA, giant	No	No	Yes	Onyx20/none	1	0 (NA)	No	Yes	No	No
42, R sc ICA, large	No	No	Yes	Onyx20/none	1	2 (H)	No	Yes	No	Yes

* Patients 13 and 14 died after receiving the treatment relevant or irrelevant to the endovascular therapy. Aneurysms in the following patients contained previously placed GDCs: 14 (basilar tip aneurysm), 19, 21, 38. Abbreviations: cav indicates cavernous segment; p, petrous; pcav, petrocavernous segment; sc, supraclinoid; and sub cb, superior cerebellar artery.

† In patient 22, edema around the aneurysm increased after treatment.

‡ Onyx16 indicates 16% Onyx (16% EVOH, 84% DMSO); Onyx20, 20% Onyx (20% EVOH, 80% DMSO); and S, stent.

§ In the following patients, the aneurysm was not completely filled with the polymer, as shown on the posttreatment CT scans: 1, 11, 12, 16, 19, 21, 22, 27, 28, 30. That is, the polymer was not cast in the exact shape of the aneurysm.

‖ Data in parentheses are the MR appearances. H indicates hypointense; NA, not applicable because MR studies were not available; NI, not identified due to the small size; and M, mixed signal intensity.

¶ Lesions appearing after treatment. CCF indicates caroticocavernous fistula; WS, watershed.

Follow-up angiography performed in the third month and/or at 1 year. (Simultaneous control examinations for sectional imaging were performed within 2 days.) No indicates that selective angiography had not been performed yet or that images were not available. That is, the treatment was recent and control imaging had not yet been performed or the patient had refused. Two patients died after treatment and did not undergo control angiography.

** Recanalization detected during selective control angiography.

†† In the following patients, MRAs showed that the parent artery had decreased in diameter: 1, 2, 5, 8, 12, 26, 28, 40. In the following patients, MRAs, showed that the parent artery had no apparent signal intensity: 15, 17, 32, 38. In the following patients, MRA results were comparable to those of selective angiography: 3, 6, 7, 9, 17, 22, 30, 31, 34, 37, 42.

likelihood of regrowth or recurrence. Therefore, the aim of this study was to define the imaging features of the polymer-filled aneurysms and to determine the implications of these findings in follow-up. (The treatment technique and results, including complications and recurrence, were beyond the scope of this study, and these data have already been published in a select subgroup of patients [14]).

Methods

In this prospective study, CT and/or MR images of 42 patients were evaluated in correlation with the angiographic results. The patients were from two centers, and their intracranial aneurysms were treated with endosaccular casting with Onyx. Thirty-one of the patients were women and 11 were men. Their age range was 6–81 years, with a mean age of 43.7 years.

The patient group had 58 intracranial aneurysms; nine patients had multiple aneurysms. In the 42 patients, a total of 46 intracranial aneurysms were treated by using the polymer. Other aneurysms (not included in this study) were treated with Guglielmi detachable coils (GDCs) (n = 4), trispan with GDCs (n = 1), stents with GDCs (n = 1), and surgical clips (n = 2). Some were left untreated for further follow-up (n = 4). Except for three aneurysms (one basilar tip and two superior cerebellar artery aneurysms), the other polymer-treated aneurysms all originated from internal carotid artery (ICA). Of these, 26 were located on the right, and 17, on the left. Twenty-one were located at the supraclinoid segment, and the remaining 22 aneurysms involved the petrous and/or cavernous portion of the ICA. The aneurysms were 2–45 mm in their largest diameter. Among the aneurysms, 18 were giant (≥2.5 cm), 15 were large (1−2.5 cm), and 13 were small (<1 cm). Only five patients (one with two aneurysms) were treated in the acute stage of subarachnoid hemorrhage. The remainder were either asymptomatic or had headaches, vision loss, diplopia, and/or symptoms due to mass effect. Nine of the patients had prior trauma.

In seven patients, therapy had been attempted before polymer treatment. However, the treatment attempt failed or the aneurysm had recanalized at follow-up. Therefore, four aneurysmal sacs contained previously placed GDCs.

Onyx is a biocompatible polymer of EVOH dissolved in its organic solvent, DMSO. Tantalum powder is added to the polymer-solvent mixture to provide the necessary radiopacity. In this study, 16% Onyx (16% EVOH, 84% DMSO) was used in the first nine aneurysms, two of these received further treatment with 20% Onyx (20% EVOH, 80% DMSO) in a second session. In the remaining aneurysms, 20% Onyx was used.

After angiographic workup, two guiding catheters were introduced by using bilateral femoral approach. A polymer-compatible balloon catheter (Equinox; Micro Therapeutics, Inc) was first placed across the aneurysm neck, and then the polymer-compatible microcatheter (Rebar; Micro Therapeutics, Inc) was placed in the aneurysmal sac. Onyx was carefully injected under the protection of the balloon catheter until the aneurysmal sac was completely filled. Before the aneurysmal sac was filled, a stent was placed across the aneurysm neck either primarily (13 of 17 patients) or in the retreatment session (four of 17 patients); this was done because of the recanalization of aneurysms initially treated with the polymer alone. In all cases, balloon-expandable, stainless steel stents were used, with polymer-compatible balloon (S670 AVE; Medtronic, Inc, Minneapolis, MN). The length was selected according to the width of aneurysm neck to provide full coverage of the neck. The stent was first placed across the aneurysm neck, and the balloon of the stent was left in place to serve as a protective device. Afterward, the polymer-compatible microcatheter was introduced; it passed through the struts of the stent, and the polymer was administered in small quantities. The technical details are described in another article (14).

A total of 81 CT and 79 MR images were evaluated. All patients but four had undergone at least one sectional imaging examination in their preprocedural evaluation. After the treatment, CT was performed in 36 patients, and MR imaging, in 32 patients. MR angiograms (MRAs) were available in 22 patients, one with two aneurysms treated with the polymer. CT examinations were performed by using several scanners (Philips AVEI Tomoscan, Rotterdam, the Netherlands; Somatom Volume Zoom, Siemens, Erlangen, Germany; and QXI Lightspeed, GE Medical Systems, Milwaukee, WI). MR imaging examinations were performed by using a 0.5-T unit (NT-Intera; Philips) and/or a 1.5-T unit (Symphony, Siemens; Magnetom SP 4000, Siemens; or Horizon Echospeed, GE Medical Systems). The primary author (I.S.) and additional investigators at each center (H.S.C. in Hacettepe University, Ankara, Turkey, and E.F.M.C. and M.E.M. at Methodist Hospital, Houston, TX) analyzed the hard-copy images.

The follow-up protocol included selective angiography in the third month and at 1 year. In 35 patients with 38 aneurysms, one or more follow-up angiographic studies were obtained in correlation with CT and/or MR imaging.

CT scans were evaluated for the presence of calcification and/or thrombus, unless the aneurysmal sac was too small to be identified on the preoperative CT images. In the postinterventional examination, the degree to which the polymer filled the aneurysm sac, complete or incomplete, was defined. Artifacts caused by the material were noted, and whether they precluded sufficient evaluation of the images was determined. Any lesion occurring after the intervention was also noted.

MR examinations included turbo spin-echo T2-weighted and gradient-echo (GRE) T2-weighted, spin-echo T1-weighted, and fluid-attenuated inversion recovery sequences with 20 transverse sections. The 5-mm-thick sections were chosen so that the 11th image was through the line from the posterior commissure to the anterior commissure; this was done to obtain comparable images at the same levels. In many patients, MRA was also performed by using a phase-contrast technique with 30-cm/s velocity encoding and/or a 3D time-of-flight technique. On MR images, the signal intensity of the aneurysm before and after treatment was defined as hyperintense, isointense, or hypointense with reference to the white matter. The homogeneous or heterogeneous appearance of the aneurysm and the presence of pulsation and magnetic susceptibility artifacts, if present, were noted. New lesions appearing after treatment were carefully recorded for possible intervention-related events, even if the patient was asymptomatic or if the lesion was in an irrelevant vascular territory. The patency of the parent artery, with any possible compromise of its caliber, was noted. The patency of the parent artery and possible neck remnants on the immediate control MRA were investigated, and recanalization and regrowth were assessed in the follow-up examinations. During the follow-up examinations, any interval change was noted. MR results were then correlated with the findings from selective angiography.

The Table shows the data regarding the size, location, and features (calcification, thrombus, mass effect) of the aneurysms; treatments; and results of control and follow-up examinations (CT, MR imaging, MRA, selective angiography).

Results

CT Findings

Seven aneurysms had calcification in the aneurysm wall; all of these were giant aneurysms (Fig 1). All except one had thrombus formation in the aneurysm

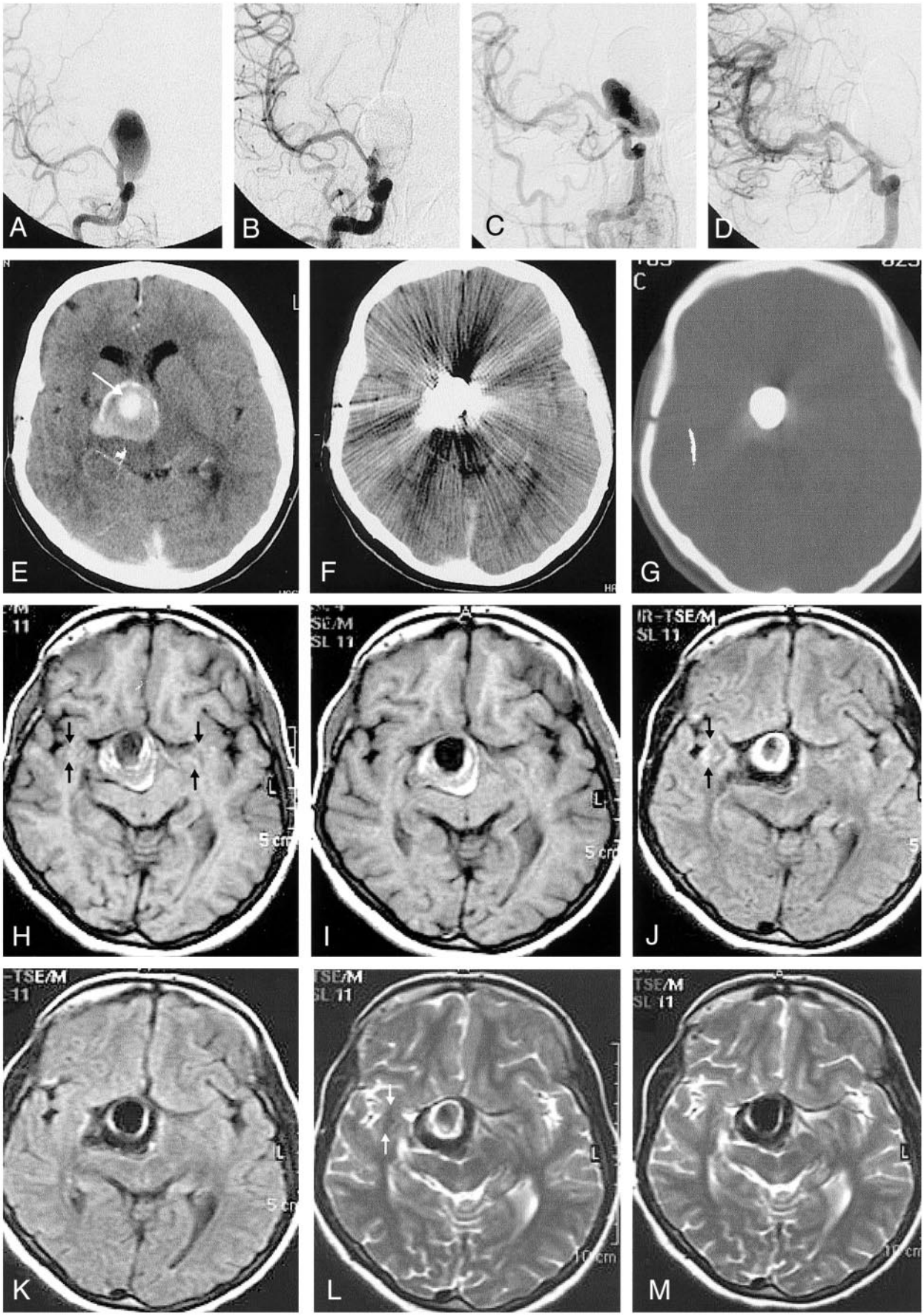
A
B
C
D
E
F
G
H
I
J
K
L
M

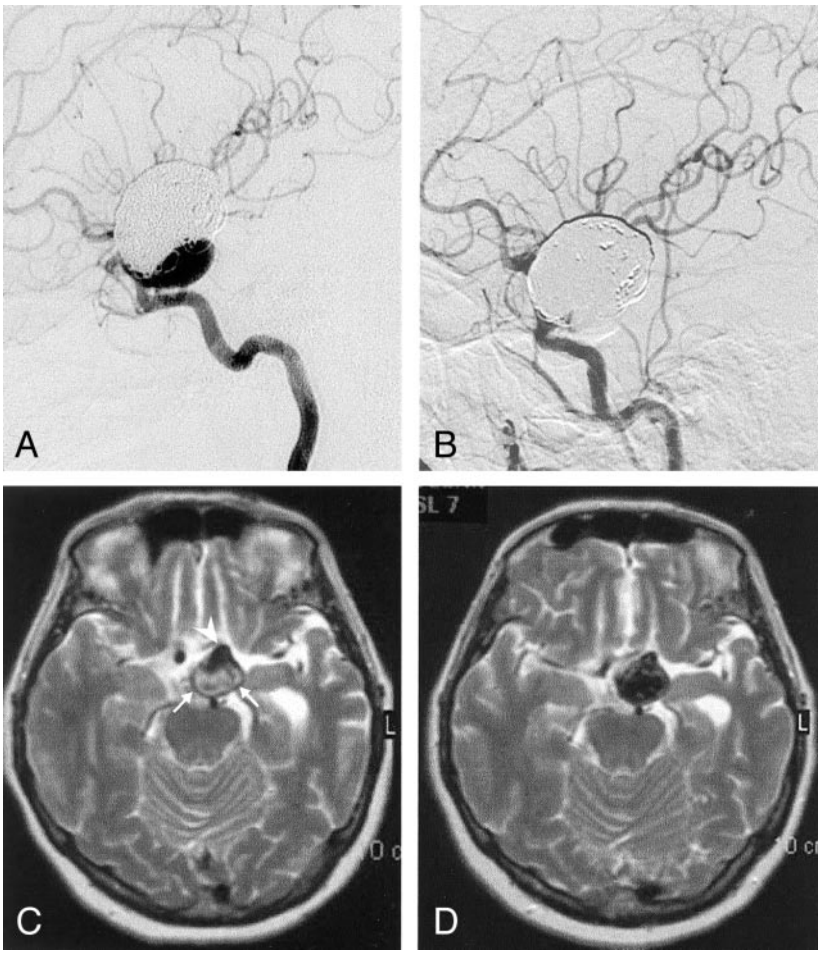

FIG 2.
A, Lateral left internal carotid angiogram reveals partial recanalization of the giant left ICA aneurysm that had been initially treated with GDC occlusion.
B, Left internal carotid right oblique angiogram after polymer treatment shows that the regrowth at the neck is completely occluded.
C and *D*, Axial T2-weighted turbo spin-echo MR images before (*C*) and after (*D*) polymer treatment. The entire aneurysm sac is hypointense after being filled; this finding includes the hypointense patent regrowth (*arrowhead*) and the thrombosed portion containing the GDC (*arrows*). The signal intensity change in the thrombosed portion may suggest penetration of the polymer into the coil mass and thrombus.

sac. Additionally, partial thrombosis of the aneurysm occurred in five other patients, two of whom had prior GDC treatment (Figs 2 and 3).

On the postprocedural CT scans, almost all of the aneurysms treated with the polymer created attenuating streak artifacts; the three small aneurysms were exceptions (Figs 1 and 3). The artifact did not allow evaluation of the adjacent brain parenchyma, and when needed, an investigation of the subarachnoid hemorrhage on the subsequent sections was not possible. The cast of the polymer was better appreciated on the images obtained with bone settings. In 10 aneurysms, the cast did not entirely fill the aneurysm sac (Figs 1 and 3). Five showed recanalization at follow-up, whereas four remained stable; one patient did not undergo follow-up examination. The recanalization rate in this group of patients was 50%, which was higher than the 21% (eight of 38) in the entire group who underwent control angiography. Therefore, the shape of the cast with respect to aneurysm sac (the degree of filling) may indicate the possibility of recanalization. We did not observe any interval change in the shape of the cast on control CT scans or selective angiograms.

←
FIG 1.
A, Pretreatment angiogram demonstrates partially thrombosed giant right ICA aneurysm.
B, Immediate posttreatment angiogram shows obliteration of the aneurysm sac with minimal filling, if any, at the neck.
C, Follow-up angiogram reveals regrowth at the neck of the aneurysm.
D, Control angiogram after retreatment with the stent and the polymer shows complete obliteration of the aneurysm.
E, Pretreatment contrast-enhanced CT image demonstrates partially thrombosed giant aneurysm with the patent portion of the aneurysm enhancing (arrow). Note the calcification at the aneurysm wall.
F and *G*, Nonenhanced CT images obtained after initial treatment with parenchyma (*F*) and bone (*G*) settings. Attenuating streak artifact hinders the evaluation of the parenchyma. With the bone setting, the attenuating cast of the polymer is seen extending beyond the patent portion; this finding indicates the extension of the material into the thrombus, though it does not completely fill the sac.
H and *I*, Corresponding T1-weighted images before (*H*) and after (*I*) treatment. The images differ in regard to the loss of pulsation artifact (*arrows*) and the increased hypointensity in the occluded nonthrombosed portion of the aneurysm after treatment.
J–M, Fluid-attenuated inversion recovery images (*J*, *K*) and T2-weighted turbo spin-echo images (*L*, *M*) demonstrate disappearance of the pulsation artifact (*arrows*). *J* and *L* were obtained before treatment, and *K* and *M*, after treatment. The hyperintense interface between the thrombosed portion and the lumen of the patent aneurysm appears thinner, possibly because of the absence of flow and consequent turbulence after treatment. Otherwise, the polymer itself does not create any signal intensity. No change in mass effect and no edema are observed after treatment.

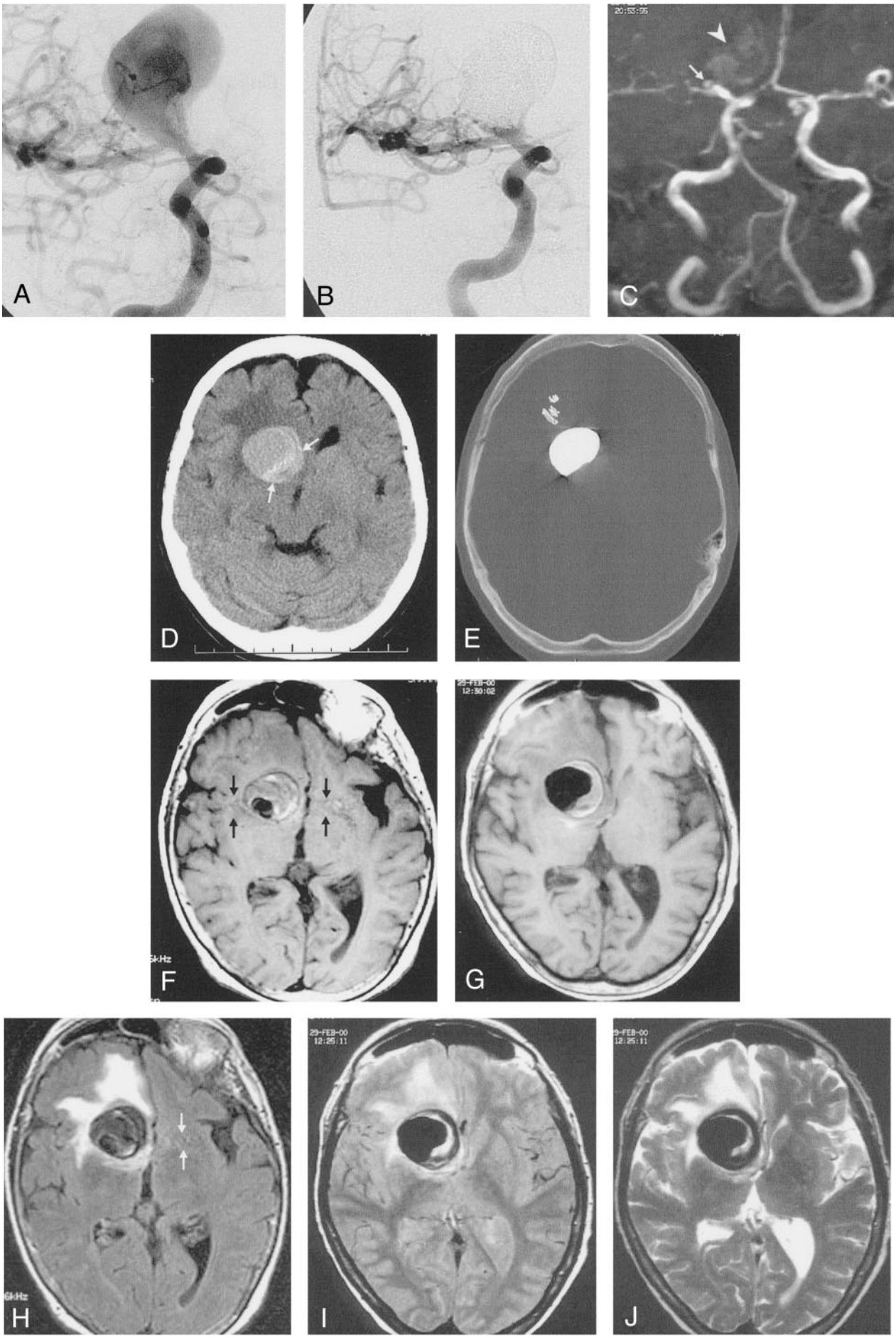
A
B
C
D
E
F
G
H
I
J

MR Imaging and MRA Findings

On MR images, regardless of the sequence used, the polymer itself appeared hypointense (Figs 1–5). However, the appearance of the aneurysm varied depending on its content (eg, thrombus [Figs 1 and 3], calcification [Fig 1], or any additional embolic material [GDC, stent, Fig 2]) within the sac itself or nearby and/or depending on the flow into the sac. Therefore, depending on the size of the aneurysm, various MR imaging appearances were noted after the polymer treatment. Aneurysms showed mainly two distinct patterns (Fig 6): hypointense to white matter with all sequences (13 aneurysms) or mixed signal intensity (16 aneurysms) (Figs 1 and 3). A diffuse hypointense pattern was seen in all small aneurysms; those can be identified on MR images (five of 13) and in six of 13 large and two giant aneurysms (Figs 4 and 5). Four small aneurysms could not be identified on MR images. When compared with the preprocedural images, the postprocedural images showed hardly any difference in the part of the sac that had a flow void after occlusion with the polymer. That is, these areas remained hypointense after treatment, but in some cases, the hypointensity became homogeneous or augmented. However, turbulent flow had been within the sac (especially in the large or giant aneurysms), the heterogeneity due to turbulent flow disappeared in those aneurysms; the result was the appearance of a hypointense sac with all sequences (Fig 4). In a few patients, the hypointensity on the pretreatment MR images (which represented the patent lumen of the aneurysm) extended into the heterogeneously intense portion of the aneurysm (which represented the thrombus) after treatment. This finding was due to the penetration of the polymer into the thrombus (Figs 2 and 3). However, in the small aneurysms with an already hypointense appearance, pretreatment images were difficult to differentiate posttreatment images (Fig 5).

In no patients did the polymer create any artifact on MR images, including the GRE images (Figs 4 and 5). Another finding was the disappearance of pulsation artifact after the treatment (Figs 1 and 3), if it had been present on the pretreatment images. In two aneurysms, pulsation artifacts persisted despite treatment; however, in both, the polymer did not completely fill the sac.

In 14 of 15 aneurysms (three large and the rest giant), the pretreatment mass effect (Fig 1) and any surrounding edema (Fig 3) did not increase. The only exception was a patient who underwent repeat treatment with the polymers and stents because recanalization had occurred after initial treatment. After this second session, parenchymal edema developed around the aneurysm, and mass effect and the prior hydrocephalus increased as well.

In 12 patients, new lesions appeared on the posttreatment examinations. (Two patients underwent only CT examinations.) Three patients had cerebellar ischemic lesions; one received treatment for the ipsilateral superior cerebellar artery aneurysm. In the other two patients, who had ICA aneurysms, the vertebrobasilar system was not even catheterized. Therefore, the pathogenesis of the lesions could not be explained. In one patient who had a cavernous ICA aneurysm, a caroticocavernous fistula developed at the end of the procedure, and the relevant cranial nerve findings were noted. However, the symptoms resolved in a week's time without any intervention, and the results of control angiography performed before the patient's discharge were normal. In three patients, ischemic lesions were present in the watershed distribution in the ipsilateral hemisphere. We noted small cortical lesions in two patients and multiple, tiny, white matter lesions in two other patients. Among these patients, two had additional basal ganglial lesions. Overall, only two of the patients with ischemic lesions had a relevant neurologic abnormality. The remaining patient had subarachnoid and parenchymal hemorrhage and eventually died; this was the only procedure-related mortality.

On MRAs obtained after treatment, the lumen of the ICA either appeared narrow (eight of 22), or it did not appear at all (three of 22) on reconstructed maximum intensity projection images. However, the patency of the vessel was confirmed with conventional angiography. In nine, stents had been placed (Fig 7). The two remaining aneurysms were giant aneurysms; mass effect may have caused the narrowed appearance of the vessel. However, on the raw images, the

←

FIG 3.

A and *B*, Right internal carotid angiograms obtained before (*A*) and after (*B*) treatment. Images show that the partially thrombosed giant right ICA aneurysm is almost completely occluded; it has a small residual neck.

C, Time-of-flight MRA successfully demonstrates the neck residuum (*arrow*). Note the slight hyperintensity due to thrombus in the region of giant aneurysm (*arrowhead*).

D, Pretreatment nonenhanced CT image shows the partially thrombosed giant aneurysm with surrounding edema and mass effect. *Arrows* indicate the thrombosed portion.

E, Posttreatment CT image (bone settings) shows that the attenuating cast of the polymer fills the aneurysm sac, except for the thrombosed portion.

F–J, Axial MR images through the same level shows the hypointensity of the aneurysm lumen becomes more prominent. The hypointensity extends into the isointense or hyperintense thrombosed portion after treatment; this may indicate the insinuation of the polymer into the thrombus in the sac. The edema and mass effect of the aneurysm persist but do not increase after treatment.

F, Pretreatment T1-weighted image. Note the pulsation artifact with the same caliber as the patent portion (*arrows*).

G, Posttreatment T1-weighted image.

H, Pretreatment fluid-attenuated inversion recovery image.

I, Posttreatment proton density–weighted image. The artifact disappears on this corresponding image.

J, Posttreatment T2-weighted turbo spin-echo image.

FIG 4.

A and *B*, Pre- and posttreatment angiograms demonstrating large ICA aneurysm occluded completely

C–J, Corresponding pre- and posttreatment T1-weighted (*C, D*), fluid-attenuated inversion recovery (*E, F*), turbo spin-echo (*G, H*), and GRE (*I, J*) T2-weighted MR images. On the pretreatment images, the left ICA aneurysm shows increased signal intensity due to slow flow (*arrow*, *C*, *E*, *G*, *I*). After it was filled with the polymer, the aneurysm appears homogeneously hypointense; the appearance resembles the signal void of a patent aneurysm.

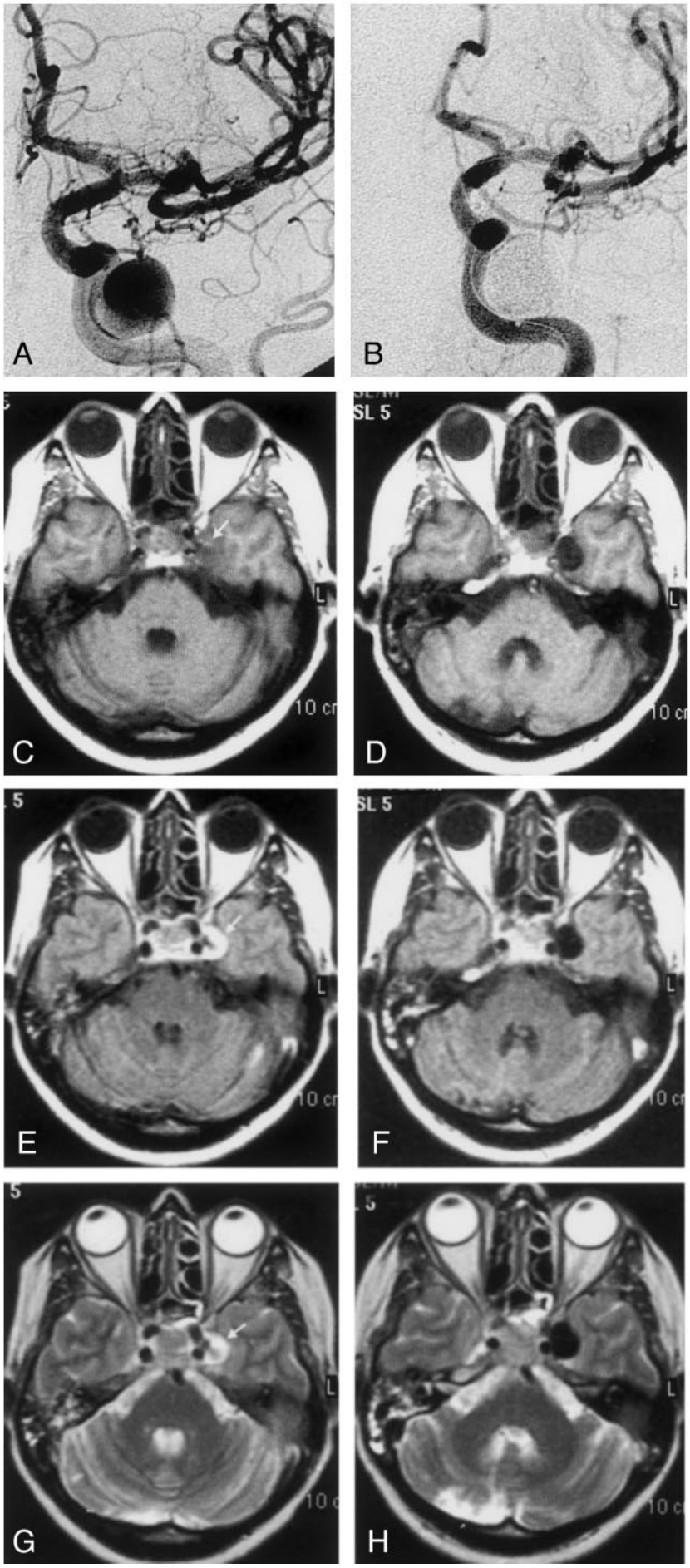

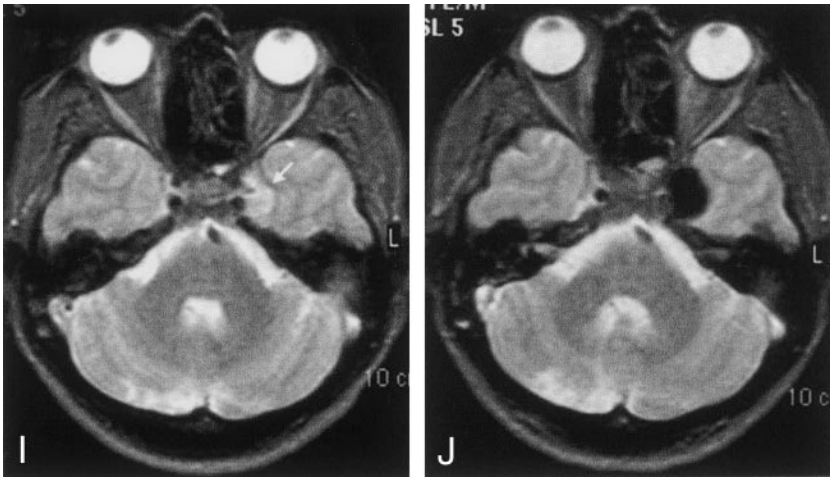

FIG 4. Continued

lumen could be appreciated with its uncompromised caliber. In the remaining 11 of 22 patients (with 12 aneurysms, all without stents and including one with an occluded ICA), MRA provided satisfactory images. These images were comparable to the selective angiograms (Figs 3 and 5). We had only three aneurysms that recanalized and that had been studied with simultaneous MRA; for these, MRA provided com-

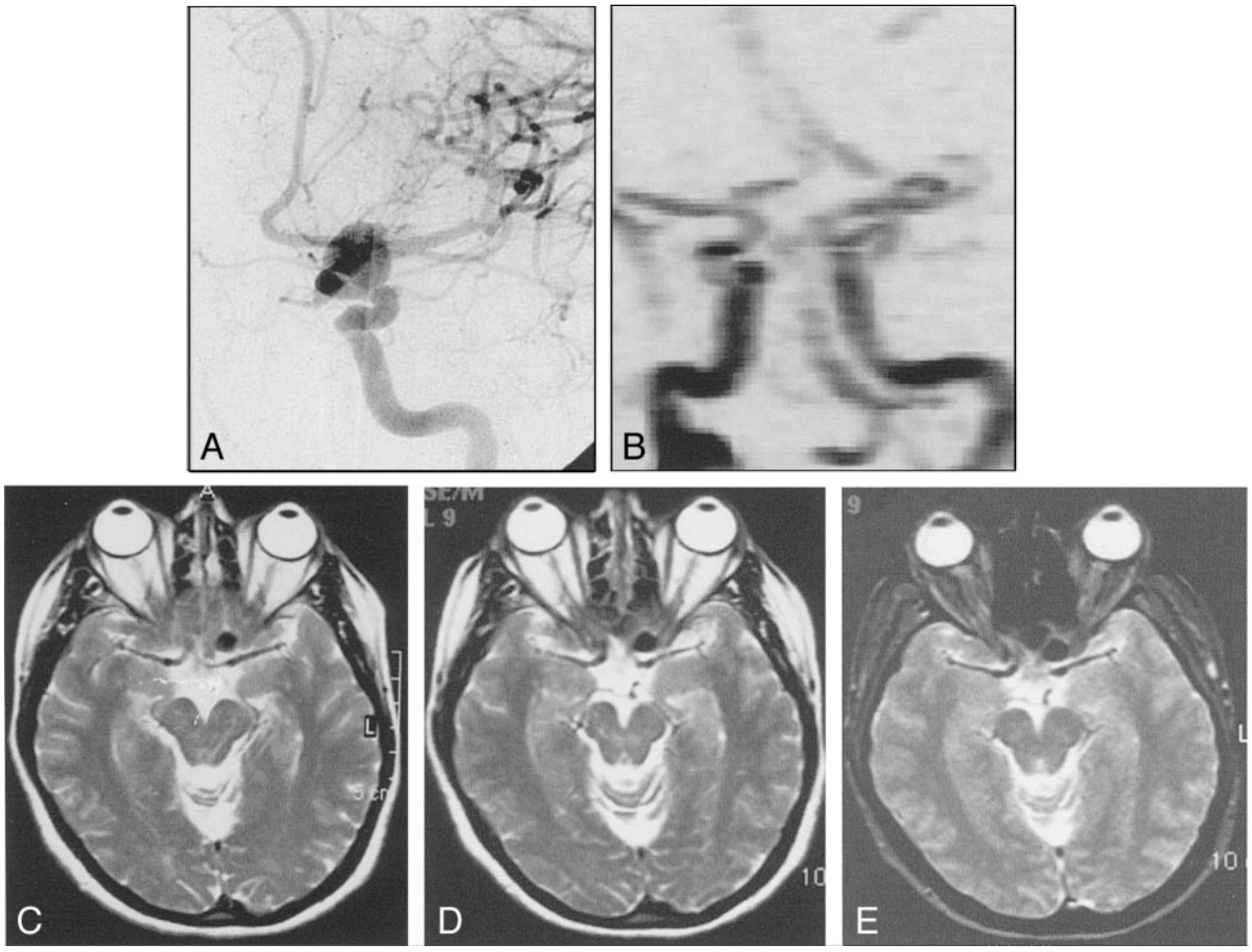

FIG 5.

A, Pretreatment angiogram demonstrates the left ICA aneurysm.

B, Phase-contrast MRA obtained after treatment shows occlusion of the aneurysm with no compromise of the parent artery. The polymer does not create any artifact that hinders the application of MRA.

C–E, Corresponding pretreatment T2-weighted turbo spin-echo (*C*), posttreatment T2-weighted turbo spin-echo (*D*) and GRE (*E*) MR images show the hypointense aneurysm. It has an identical appearance before and after treatment that is not possible to appreciate if the aneurysm is patent.

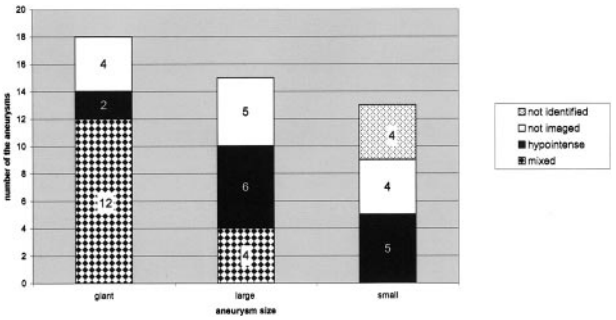

FIG 6. MR imaging appearances of the aneurysms. Graph shows the distribution according to aneurysm size.

parable results. However, the number of patients with recanalization and the simultaneous studies available for comparison were not sufficient. As a result, we could not comment on the effectiveness of MRA in detecting recanalization in the presence of the polymer, with or without stents.

Discussion

Endosaccular coiling has an established role in the treatment of intracranial aneurysms worldwide (1, 2, 7, 15). Nevertheless, the effectiveness of the method and long-term follow-up data (including the rates of recanalization and bleeding) is still being determined in ruptured and unruptured aneurysms (8, 9). Therefore, immediate control and also follow-up is important in these patients. Conventional angiography is the criterion standard for the evaluation of treated intracranial aneurysms; however, the role of noninvasive techniques such as MR imaging (including diffusion imaging), MRA, CT angiography, and even Doppler sonography in the immediate postprocedural period and in follow-up has been the subject of investigations (16–23).

The MR safety of the GDCs has been documented (24–25), and the MR appearance of GDCs has also been described (25). GDCs were observed to produce minor distortion on the MR images, and the artifacts were localized to the area of coil. Therefore, such artifacts do not greatly affect the diagnostic aspects of MR imaging (25). Many authors have reported comparable results with MRA in the follow-up of GDC-treated aneurysms (18, 19, 21).

Because Onyx is an embolic agent that has recently come into use, its CT and MR appearances have not been described in the literature. To our knowledge, the published reports describe experimental studies, the technique (including its safety and efficacy), or the patients with Onyx-treated AVMs (12, 13, 14, 26), with no description of the imaging features and their implications. On MR images, regardless of the se-

FIG 7.
A and *B*, Post-treatment subtracted (*A*) and nonsubtracted (*B*) selective angiograms of the right ICA show complete occlusion of the aneurysm. A dense cast of the polymer fills the aneurysm. The parent artery is patent.
C and *D*, Time-of-flight (*C*) and phase-contrast (*D*) MRAs show complete occlusion of the giant aneurysm. The parent artery is patent but markedly narrowed (*arrows*) due to the presence of the stent, which results in a signal intensity loss.

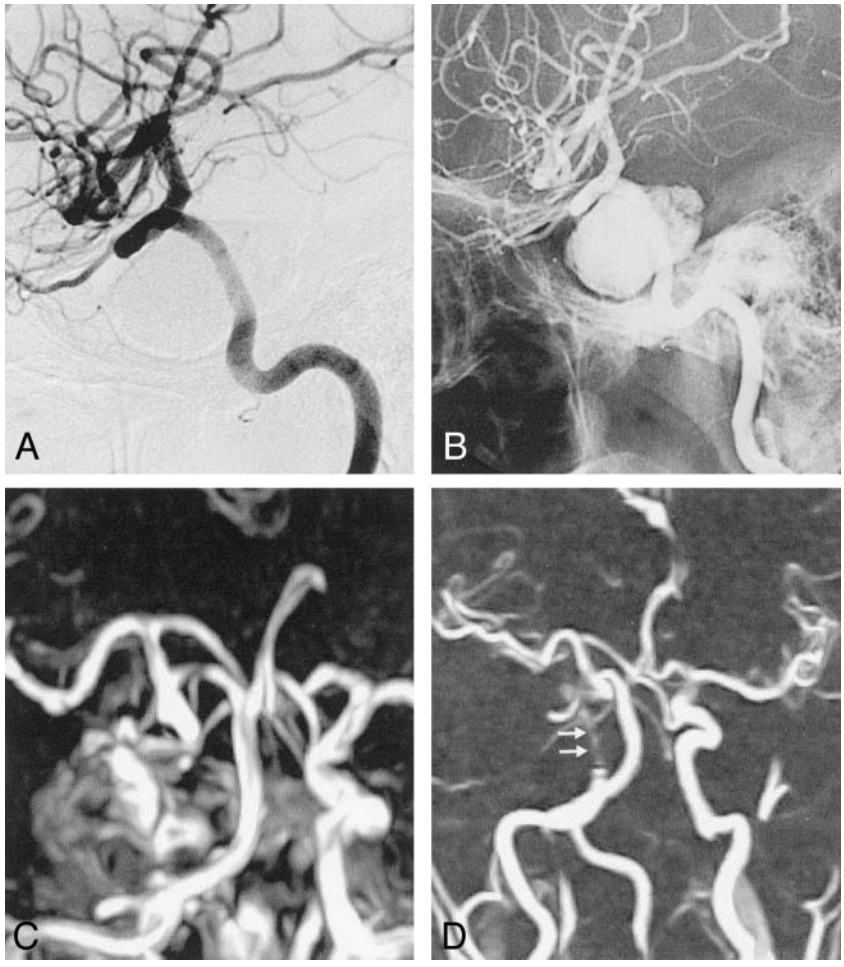

quence used, the appearance of the polymer-filled aneurysms did not change appearance apart from the flow effects. Therefore, we understand that Onyx itself appears hypointense (Figs 1–5), despite the lack of in vitro studies. Tantalum intravascular devices have been shown to cause flow voids, or hypointense appearance, on MR images. They result in only negligible magnetic susceptibility artifacts, if any, as described in previous reports (27, 28). We attribute the persistent hypointensity of the Onyx–filled aneurysms to its tantalum content. Because tantalum is nonferromagnetic, Onyx did not create any artifact on MR images, even on GRE images (Figs 4J and 5E), which are more sensitive to the magnetic susceptibility. It did not spoil the diagnostic quality of MRAs, and MRA provided results comparable to those of simultaneous conventional angiography (Figs 3 and 5). On the other hand, on MRAs in patients with auxiliary stents, the parent artery appeared narrow, and this finding is attributed to the signal intensity loss caused by the stainless steel stent (Fig 7). Stainless steel is known to cause metallic artifact and signal intensity drop-out, resulting in a black-hole appearance on MR images; they also hinder the depiction of intraluminal signal intensity on MRAs (27, 29, 30). In our series, reconstructed MRAs in only two of the patients without stents falsely suggested parent-artery narrowing; this result was probably due to mass effect of the aneurysms, as both of the aneurysms were giant.

Another MR feature of the polymer-filled aneurysms was the vanishing of heterogeneity in some cases; this was most likely due to the disappearance of flow effects in the fully occluded aneurysm sac (Fig 4). The pulsation artifact recognized on pretreatment images disappeared (Figs 1 and 3) after the aneurysm was occluded with the polymer. In two patients who had incomplete filling of the aneurysm, the pulsation artifact persisted on posttreatment images; these aneurysms showed further recanalization in the control examination. Therefore, the persistence of pulsation artifacts after treatment may indicate flow within the aneurysm and future recanalization.

On CT scans, the polymer filling the aneurysm created attenuating streak artifact (Fig 1). This finding is consistent with those of the previous reports about the CT features of several tantalum devices (30–32). In our series, incomplete filling of the aneurysm sac was more likely to be associated with recanalization at follow-up than with completely filled aneurysm sacs, though the shape of the cast did not change in the time interval. Therefore, in this group of patients, one should be cautious during follow-up.

Another issue was the evaluation of the posttreatment change in mass effect and edema caused by the polymer-filled aneurysm. Onyx filling did not create any observable change in the volume of the aneurysm, as shown on sectional images. Aggravation of the symptoms of mass effect after GDC packing has been reported (33, 34). In our series, no patients (including 15 with mass effect on pretreatment studies) developed new symptoms due to mass effect or had an aggravation of preexisting symptoms. These findings paralleled those of the imaging studies, which showed no posttreatment change (Figs 1 and 3). An exception was one patient who had increasing edema after the second treatment session; this patient had adjunctive stent, and the edema resolved in time. Therefore, one may conclude that filling of the aneurysm with the polymer did not cause any increase in mass effect; still, one may presume otherwise because of the possible increase in the volume of the aneurysm, at least in the immediate postprocedural period.

The procedure-related adverse events for endovascular treatment techniques have been evaluated (35). Symptomatic or asymptomatic thromboembolic events may occur as a complication of GDC treatment (22, 36). Diffusion-weighted MR imaging reveals silent ischemic lesions, even in unrelated vascular territories. Rordorf et al (36) reported that the rate of asymptomatic emboli is 61% in uncomplicated GDC treatments. In our group, despite lack of diffusion weighted MR imaging (which is more sensitive), MR imaging revealed new ischemic lesions that developed after treatment. These were observed in 10 (31%) of 32 patients who underwent posttreatment MR imaging, and only two of them were symptomatic. Two patients had ischemic lesions of unclear cause in the irrelevant vascular territory (ie, cerebellar hemispheres) despite the fact that the intervention had been confined to the ICA. Three patients had watershed lesions, which may be attributable to the balloon protection during the procedure. The small cortical lesions and multiple, tiny, white matter lesions may have resulted from thromboemboli despite meticulous heparinization during the procedure; however, the pathogenesis of these lesions is not proved. The angiotoxicity of this embolic agent has been investigated (10, 37) since its original development (11). The slow injection of a certain volume at a time has been recommended to prevent this possibility. Jahan et al (12) reported angionecrosis of the embolized vessels on histopathology in their AVM group with no neurologic deficit. Angiotoxicity may also be questioned in the etiology of the previously mentioned parenchymal lesions. However, despite the lack of histopathologic proof, we do not think that this possibility is likely because the injections were slow and limited in volume. This aspect had already been thoroughly investigated before clinical application.

Conclusion

The new liquid embolic agent, Onyx, appears hypointense on MR images, regardless of the sequence used. It produces no artifacts, and it did not interfere with MRA applications. As a result, MRA provides results comparable with those of conventional angiography, unless stainless-steel adjunctive stents have been placed; these can cause a loss of signal intensity. On CT scans, the polymer creates attenuating streak artifacts, and the surrounding parenchyma may not be adequately evaluated. The treatment does not seem to cause or aggravate mass effect; this observation parallels the lack of volume change after treatment.

However, parenchymal lesions, even those in irrelevant vascular territories, may be seen in some cases, and these are not necessarily associated with relevant clinical symptoms.

4. Finally, we may recommend MR imaging and MRA for the immediate postprocedural control and follow-up of patients, and conventional angiography may be reserved for patients in whom MRA shows equivocal results, apparent regrowth, or residual aneurysms.

References

1. Gobin YP, Vinuela F, Gurian JH, et al. Treatment of large and giant fusiform intracranial aneurysms with Guglielmi detachable coils. *J Neurosurg* 1996;84:55–62
2. Vinuela F, Duckwiler G, Mawad M, et al. **Guglielmi detachable coil embolization of acute intracranial aneurysm: perioperative anatomical and clinical outcome in 403 patients.** *J Neurosurg* 1997;86:475–482
3. Akiba Y, Murayama Y, Vinuela F, Lefkowitz MA, Duckwiler GR, Gobin YP. **Balloon-assisted Guglielmi detachable coiling of wide-necked aneurysms, I: experimental evaluation.** *Neurosurgery* 1999;45:519–530
4. Aletich VA, Debrun GM, Misra M, Charbel F, Ausman JI. **The remodeling technique of balloon assisted Guglielmi detachable coil placement in wide-necked aneurysms: experience at the University of Illinois at Chicago.** *J Neurosurg* 2000;93:388–396
5. Wakhloo AK, Lanzino G, Lieber BB, Hopkins LN. **Stents for intracranial aneurysms: the beginning of a new endovascular era?** *Neurosurgery* 1998;43:377–379
6. Phatouros CC, Sasaki TSJ, Higashida RT, Malek AM, Meyers PM, Dowd C, Halbach VV. **Stent- supported coil embolization: the treatment of fusiform and wide-neck aneurysms and pseudoaneurysms.** *Neurosurgery* 2000;47:107–115
7. Gruber A, Killer M, Bavinzski G, Richling B. **Clinical and angiographic results of endosaccular coiling treatment of giant and very large intracranial aneurysms: a 7-year, single-center experience.** *Neurosurgery* 1999;45:793–804
8. Byrne JV, Sohn MJ, Molyneux AJ, Chir B. **Five year experience in using coil embolization for ruptured intracranial aneurysms: outcomes and incidence of late rebleeding.** *J Neurosurg* 1999;90:656–663
9. Hayakawa M, Murayama Y, Duckwiler GR, Gobin YP, Guglielmi G, Vinuela F. **Natural history of the neck remnant of a cerebral aneurysm treated with the Guglielmi detachable coil system.** *J Neurosurg* 2000;93:561–568
10. Murayama Y, Vinuela F, Ulhao A, et al. **Nonadhesive liquid embolic agent for cerebral arteriovenous malformations: preliminary histopathologic studies in swine rete mirabile.** *Neurosurgery* 1998;43:1164–1175
11. Taki W, Yonekawa Y, Iwata H, Uno A, Yamashita K, Amemiya H. **A new liquid material for embolization of arteriovenous malformations.** *AJNR Am J Neuroradiol* 1990;11:163–168
12. Jahan R, Murayama Y, Gobin YP, Duckwiler GR, Vinters HV, Vinuela F. **Embolization of arteriovenous malformations with Onyx: clinicopathological experience in 23 patients.** *Neurosurgery* 2001;48:984–997
13. Murayama Y, Vinuela F, Tateshima S, Vinuela FJ, Akiba Y. **Endovascular treatment of experimental aneurysms by use of a combination of liquid embolic agents and protective devices.** *AJNR Am J Neuroradiol* 2000;21:1726–1735
14. Mawad ME, Cekirge S, Ciceri E, Saatci I. **Endovascular treatment of giant and large intracranial aneurysms by using a combination of stent placement and liquid polymer injection.** *J Neurosurg* 2002;96:474–482
15. Raymond J, Roy D. **Safety and efficacy of endovascular treatment of acutely ruptured aneurysms.** *Neurosurgery* 1997;41:1235–1245
16. Derdeyn CP, Graves VB, Turski PA, Masaryk AM, Strither CM. **MR Angiography of saccular aneurysms after treatment with Guglielmi detachable coils: preliminary experience.** *AJNR Am J Neuroradiol* 1997;17:279–286
17. Gönner F, Heid O, Remonda L, et al. **MR angiography with ultrashort echo time in cerebral aneurysms treated with Guglielmi detachable coils.** *AJNR Am J Neuroradiol* 1998;19:1324–1328
18. Kähärä VJ, Seppänen SK, Ryymin PS, Mattila P, Kuurne T, Laasonen EM. **MR Angiography with three-dimensional time-of-flight and targeted maximum-intensity-projection reconstructions in the follow-up intracranial aneurysms embolized with Guglielmi detachable coils.** *AJNR Am J Neuroradiol* 1999;20:1470–1475
19. Anzalone N, Righi C, Simionato F, et al. **Three-dimensional time-of-flight MR angiography in the evaluation of intracranial aneurysms treated with Guglielmi detachable coils.** *AJNR Am J Neuroradiol* 2000;21:746–752
20. Masaryk AM, Frayne R, Unal O, Rappe AH, Strother CM. **Utility of CT angiography and MR angiography for the follow-up of experimental aneurysms treated with stents or Guglielmi detachable coils.** *AJNR Am J Neuroradiol* 2000;21:1523–1531
21. Boulin A, Pierot L. **Follow-up of intracranial aneurysms treated with detachable coils: comparison of gadolinium enhanced 3D time-of-flight MR angiography and digital subtraction angiography.** *Radiology* 2001;219:108–113
22. Biondi A, Oppenheim C, Vivas E, et al. **Cerebral aneurysms treated by Guglielmi detachable coils: evaluation with diffusion-weighted MR imaging.** *AJNR Am J Neuroradiol* 2000;21:957–963
23. Schuknecht B, Chen JJ, Valavanis A. **Transcranial color-coded Doppler sonography of intracranial aneurysms before and after endovascular occlusion with Guglielmi detachable coils.** *AJNR Am J Neuroradiol* 1998;19:1659–1667
24. Hartman J, Nguyen T, Larsen D, Teitelbaum GP. **MR artifacts, heat production, and ferromagnetism of Guglielmi detachable coils.** *AJNR Am J Neuroradiol* 1997;18:497–501
25. Shellock FG, Detrick MS, Brant-Zawadski MN. **MR compatibility of Guglielmi Detachable Coils.** *Radiology* 1997;203:568–570
26. Molyneux AJ, Coley SC. **Embolization of spinal cord arteriovenous malformations with an ethylene vinyl copolymer dissolved in dimethyl sulfoxide (Onyx liquid embolic system): Report of two cases.** *J Neurosurg* 2000;93(2 Suppl):304–308, 2000
27. Teitelbaum GP, Ortega HV, Vinitski S, et al. **Low-artifact intravascular devices: MR Imaging evaluation.** *Radiology* 1988;168:713–719
28. Matsumoto AH, Teitelbaum GP, Barth KH, Carvlin MJ, Savin MA, Strecker EP. **Tantalum vascular stents: in vivo evaluation with MR imaging.** *Radiology* 1989;170:753–755
29. Amano Y, Gemma K, Kawamata H, Kumazaki T. **Intraluminal signal intensity of iliac artery stents investigated by contrast-enhanced three-dimensional MR angiography.** *Comput Med Imaging Graph* 1998;22:9–12
30. Amano Y, Ishihara M, Hayashi H, et al. **Metallic artifacts of coronary and iliac arteries stents in MR angiography and contrast-enhanced CT.** *Clin Imaging* 1999;23:85–89
31. Wang JC, Yu WD, Sandhu HS, Tam V, Delamarter RB. **A Comparison of magnetic resonance and computed tomographic image quality after the implantation of tantalum and titanium spinal instrumentation.** *Spine* 1998;23:1684–1688
32. Levi ADO, Choi WG, Keller PJ, Heiserman JE, Sonntag VKH, Dickman CA. **The radiographic and imaging characteristics of porous tantalum implants within the human cervical spine.** *Spine* 1998;23:1245–1251
33. Litofsky NS, Vinuela F, Gianotta SL. **Progressive visual loss after electrothrombosis treatment of a giant intracranial aneurysm: case report.** *Neurosurgery* 1994;34:548–550
34. Ushikoshi S, Kikuchi Y, Houkin K, Miyasaka K, Abe H. **Aggravation of brainstem symptoms caused by a large superior cerebellar artery aneurysm after embolization by Guglielmi detachable coils-case report.** *Neurol Med Chir* 1999;39:524–529
35. Lövblad KO, Plüschke W, Remonda L, et al. **Diffusion-weighted MRI for monitoring neurovascular interventions.** *Neuroradiol* 2000;42:134–138
36. Rordorf G, Bellon RJ, Budzik RE Jr, et al. **Silent thromboembolic events associated with the treatment of unruptured cerebral aneurysms by use of Guglielmi detachable coils: prospective study applying diffusion-weighted imaging.** *AJNR Am J Neuroradiol* 2001;22:5–10
37. Chaloupka JC, Huddle DC, Alderman J, Fink S, Hammond R, Vinters HV. **A reexamination of the angiotoxicity of superselective injection of DMSO in the swine rete embolization model.** *AJNR Am J Neuroradiol* 1999;20:401–410